

This is the accepted manuscript made available via CHORUS. The article has been published as:

## Evidence of Negative-Index Refraction in Nonlinear Chemical Waves

Xujin Yuan, Hongli Wang, and Qi Ouyang

Phys. Rev. Lett. **106**, 188303 — Published 6 May 2011

DOI: [10.1103/PhysRevLett.106.188303](https://doi.org/10.1103/PhysRevLett.106.188303)

# Evidence of negative index of refraction in nonlinear chemical waves

Xujin Yuan<sup>1</sup>, Hongli Wang<sup>1,2</sup>, Qi Ouyang<sup>1,2</sup> \*

<sup>1</sup>*State key Laboratory for Mesoscopic Physics,*

*Department of Physics, Beijing 100871,*

*China* <sup>2</sup>*Center for Theoretical Biology,*

*Peking University, Beijing 100871, China*

## Abstract

Negative index of refraction of electromagnetic waves was predicted and observed in artificial meta-materials. The same phenomenon in nonlinear chemical waves has become a recent focus in nonlinear dynamics researches. Theoretical analysis and computer simulations have predicted that negative index of refraction can occur on the interface between antiwaves and normal waves in a reaction-diffusion (RD) system. However, no experimental evidence has been found so far. In this letter, we report our experimental design in searching for such a phenomenon in a chlorite-iodide-malonic acid (CIMA) reaction. Our experimental results demonstrates that competition between waves and antiwaves at their interface determines the fate of the wave interaction. The negative index of refraction was only observed when the oscillation frequency of a normal wave is significantly smaller than that of the antiwave. All experimental results were supported by simulations using the Lengyel-Epstein RD model which describes the CIMA reaction-diffusion system.

PACS numbers: 82.40.Ck, 82.40.Bj, 47.54.-r, 89.75.Kd

---

\* To whom correspondence may be addressed. E-mail: qi@pku.edu.cn

The recent discovery of antispiral and antitarget waves in reaction-diffusion systems[1–3] has attracted much interest because of a unique characteristic: the wave’s phase velocity is opposite to their group velocity[4, 5]. A normal concentric or spiral wave in a reaction-diffusion system has outward propagation from its wave source, because its phase velocity and group velocity point to the same direction. In contrast antitarget and antispiral waves propagate inwardly towards the wave source, because the phase and group velocities are opposite. Numerous theoretical and numerical studies have been carried out to investigate this antiwave behaviors[6–8]. Among them, the refractive index of these nonlinear waves on the wave-antiwave interface is a major focus[8–10]. In a linear counterpart system such as electromagnetic waves, artificial meta-materials can be designed to have a negative value of the refractive index at the interface. This property was first predicted in the late 1960’s[11] and experimentally realized recently[12]. One of the necessary conditions for negative index of refraction is that the phase velocity of the optical waves is opposite to the group velocity. It is interesting to investigate whether a nonlinear wave behaves the same for two reasons. Theoretically, a better understanding of the behavior of nonlinear traveling waves is helpful to explain the wave propagation mechanism of other nonlinear systems, such as heart muscles and microorganisms. Practically, it is interesting to design new functional materials that have novel nonlinear wave behavior. This motivated us to systematically research wave behavior at the interface between a normal wave and an antiwave in a reaction-diffusion system.

Presently, negative index refraction in chemical waves has been predicted in numerical simulations[8–10]. Cao etc.[9] found negative index refraction at the wave-antiwave interface using CGLE and Brusselator models in RD systems. They scanned the forcing frequency to identify suitable physical conditions for negative index of refraction to occur. The relationship between the incidence and refraction angle were also discussed theoretically and numerically. A further work reported numerical exploration based on the dispersion relation of the CGLE[10], which demonstrates that the forcing frequency in the CGLE model determines wave refraction behavior at the interface. These numerical simulations attempt to survey the underlying mechanisms of negative index of refraction. However, fundamental experimental evidence in reaction-diffusion systems is still lacking.

The first step in experimentally testing negative index of refraction behavior in nonlinear chemical waves is creating a wave-antiwave interface in a RD system. Our former experimental and theoretical research found that, under certain experimental conditions, the chlorite-iodide-malonic acid (CIMA) reaction system supports antiwave formation, and the concentration of polyvinyl

alcohol (PVA), the color indicator of reaction, is a sensitive parameter for determining the wave-antiwave exchange [3, 13, 14]. Thus, with different concentrations of PVA loaded in the reaction medium, one can generate normal waves and antiwaves with the same boundary conditions. This behavior allows us to create a wave-antiwave interface in such a RD system.

Our experiments were conducted in a spatially open reactor with the CIMA reaction[13, 15, 16]. The reaction medium was a thin disk of agarose gel pre-loaded with PVA. It was sandwiched between two thin porous glass disks, which could lock PVA molecules inside the gel. The outer surfaces of the glass disks were in contact with two chemical solution reservoirs. An interface between normal wave and antiwave areas could thus be created by putting together two gel parts with different PVA concentrations. In this experiment, we fixed the concentration of PVA in the part of gel that generated antiwaves, and used the concentration of PVA in the other part of gel (normal wave part) as a control parameter. We monitored different types of wave-wave interactions at the interface and searched for evidence of negative index of refraction behavior in the nonlinear wave. The diffusion time of PVA in the gel is quite long, so the concentration of PVA in the two parts of gels can be considered constant, with the PVA concentration gradient at the interface being sharp.

The chemical concentrations of CIMA reaction in the two solution reservoirs were different and fixed in each experiment. One reservoir contained 20 *mM* sodium chlorite, 1 *mM* sodium hydroxide; the other contained 21 *mM* sulfuric acid, and malonic acid (MA). Both reservoirs contained 3.48 *mM* potassium iodide and 4.5 *mM* sodium sulfate. The concentration of PVA in the antiwave medium was fixed at 4g/L; the concentration of PVA in the normal wave area was tuned between 0.6g/L and 2.2g/L. The concentration of MA was another control parameter, which was tuned in the range from 5.7 *mM* to 6.0 *mM* (stepwise by 0.1 *mM*). Each measurement was performed when the wave behavior reached asymptotic state (the time interval was usually 2 hours).

As the control parameters were varied in sequence, we found three typical states (Fig. 1). First, the uncoupling state occurred when the concentration of PVA for the normal wave medium was between 0.6g/L and 1.0g/L. In this state the normal wave and antiwave evolved separately, so the number of wavefronts in the normal wave did not match with that of the antiwave at the interface [Fig. 1(a), movie on line]. In this situation, the interface between the normal wave and antiwave functioned like a wave sink; neither normal waves nor antiwaves could pass through. We observed the second state, the coupling state, when the concentration of PVA for the normal wave medium was increased to 1.4g/L and 1.8g/L. In this state the wavefronts of antiwave and

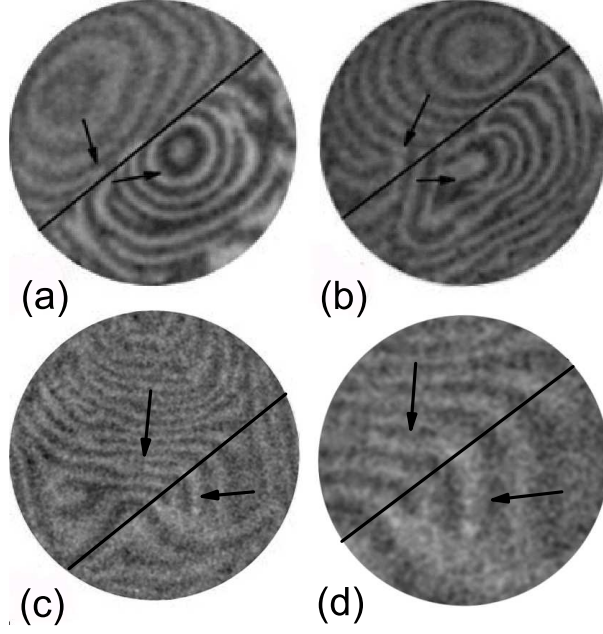


FIG. 1: Typical experimental results of the three forms of wave-wave interaction on the interface between normal wave and antiwave areas. (a),  $[MA] = 6.0\text{ mM}$ ,  $\text{PVA}=0.6\text{ g/L}$  vs  $4.0\text{ g/L}$ , the uncoupling state; (b),  $[MA] = 5.9\text{ mM}$ ,  $\text{PVA}=1.4\text{ g/L}$  vs  $4.0\text{ g/L}$ , the coupling state. (c),  $[MA] = 5.7\text{ mM}$ ,  $\text{PVA}=2.1\text{ g/L}$  vs  $4.0\text{ g/L}$ , the negative index refraction. View size diameter of (a,b,c) is  $17.6\text{ mm}$ . (d), the zoom up image of the interface of negative index refraction in (c), view size diameter of (d) is  $8.4\text{ mm}$ . The arrows indicate the direction of the phase velocities.

normal wave became coupled because the number of wavefronts matched at the interface [Fig. 1(b), movie on line]. However, the group velocities of the normal wave and antiwave both pointed to the interface, which indicated that wave refraction still did not occur. In contrast, in the third state, as the concentration of PVA for the normal wave medium was further raised to  $2.1\text{ g/L}$  and  $2.2\text{ g/L}$ , negative index refraction emerged. In this situation, the normal wave penetrated through the interface and became the source of the antiwave. The normal wave and the antiwave had a unique direction in group velocities. Whereas their phase velocities were in opposite directions; both pointed to the interface [Fig. 1(c)(d), movie online].

The experimental observations of Fig. 1 can be understood in terms of nonlinear wave competition. This is different from linear waves, which show superimposition. When two nonlinear waves meet, they collide and disappear. In order to have wave refraction on the interface, chemical waves on one side of reaction medium should pass the interface and become the wave source in the other side of reaction medium. They will face competition with waves that are already there. It

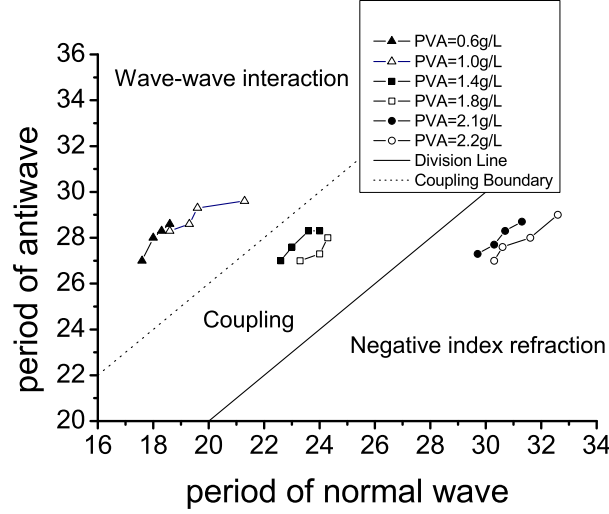


FIG. 2: Phase diagram of traveling wave behavior on the interface. The solid division line separates the negative index refraction regime and the wave sink regime. The dashed line indicates the division between the coupling and uncoupling states. Different symbols indicate different concentrations of PVA in the normal wave medium. Different concentrations of MA give different values of measured periods.

is well known that for an ordinary outwardly propagating wave, the wave with a higher oscillation frequency has an advantage. The situation is opposite in the antiwave region[3]. The reason is that, given the same wavelength, the inwardly propagating wave with the longer period takes a longer time to reach the wave center, making its survive longer. This means that a normal wave train can pass through the interface between normal wave and antiwave media only when its oscillation frequency is lower than that of the antiwave. Equally, an antiwave train can penetrate the interface only when its oscillation frequency is higher than that of the normal wave. On the contrary, a normal wave train with a higher frequency than that of the antiwave can not pass through the interface. In this case, the interface serves as a wave sink for both. Thus, the equivalent line of the oscillating periods of the normal wave and the antiwave divides the negative index refraction state and the wave-wave interaction state.

Our experiments support this qualitative reasoning. Fig. 2 is a phase diagram using measured oscillation periods of waves and antiwaves as the order parameters. The solid division line indicates where the normal wave and the antiwave are at equal periods. One observes that this line distinctly divides the negative index refraction state from the other two states. The dashed line is the boundary between the coupling and uncoupling states. The uncoupling state occurred when the discrepancy between the oscillation periods of the two waves was large. In this regime, interaction

between wave and antiwave was weak. The coupling region is in the middle of Fig. 2. Here, the frequency of the normal wave was slightly higher than that of the antiwave. In this regime the wave trains on the two sides of the interface matched. We think there might be an important interaction between the wave and antiwave at the interface. As a result, the chemical waves on both sides of the interface become resonant; they adjust their oscillation frequencies so that the wave trains on the two sides match at the interface.

To confirm our qualitative explanation about the coupling state and the negative index refraction state, the corresponding simulation was conducted. Former research confirmed that the Lengel-Epstein (LE) model can quantitatively describe the dynamics in CIMA reactions[17–20]. Since the color indicator PVA plays an important role in the antiwave formation, in this study we modified the original LE model to take the reaction of PVA into account[21]:



where  $S$ ,  $I_3^-$ , and  $C$  represent, respectively, the concentrations of PVA, tri-iodide, and PVA-iodide complex. Since the above complex formation reaction is much faster than other reactions in LE model, we assumed that it is always in a quasi-equilibrium state. Under this assumption, the non-dimensional form of Lengel-Epstein model in a RD system could be rewritten as

$$\begin{aligned} \partial x / \partial t &= \delta[a - x - 4xy/(1 + x^2)] + \delta D_x \nabla_r^2 x \\ \partial y / \partial t &= b[x - xy/(1 + x^2)] + D_y \nabla_r^2 y, \end{aligned} \quad (2)$$

where  $x$  and  $y$  are non-dimensional concentrations of  $I^-$  and  $ClO_2^-$ ;  $a$  is proportional to the concentration of MA;  $b$  is inversely proportional to  $I_2$ [22];  $\delta$  is related to the color indicator's concentration:  $\delta = 1/(1 + SK)$ , where  $K$  is the equilibrium constant of reaction (1).

According to our former theoretical study[3, 13, 14], antiwaves appear when the reaction system is just beyond the Hopf bifurcation point. When the system is moved away from the Hopf bifurcation point, antiwaves undergo a transition to normal waves. For the modified LE model, one can prove that the system undergoes a Hopf bifurcation if  $\delta > b/(3a/5 - 25/a)$ . The value of  $\delta$  determines the distance from the Hopf onset and wave-antiwave exchange. This theoretical prediction was confirmed in our experimental study.

For quantitative comparison of simulation and experimental results, the control parameters in the Eqn. (2) system were estimated from experimental conditions. In the actual experiment, the concentration of MA could be considered as constant on both the antiwave and normal wave sides,

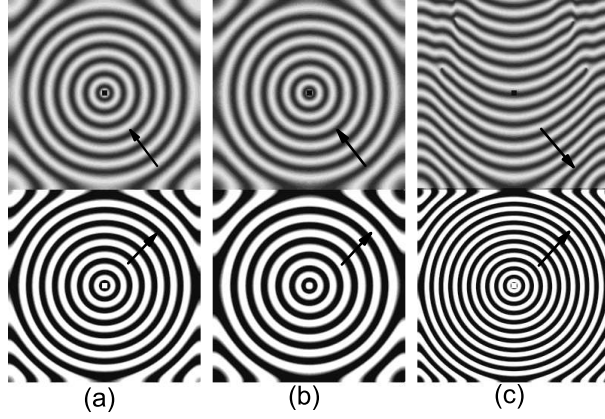


FIG. 3: Typical simulation results of the three states of wave-wave interaction at the interface between normal waves and antiwaves. The lower half of each figure is the normal wave parameter region, while the upper half is the antiwave region. (a) the uncoupling state; (b) the coupling state; (c) the negative index refraction state. The value of parameters in the upper normal wave region are respectively:  $\delta = 0.221, b = 0.32$ ;  $\delta = 0.218, b = 0.28$ ;  $\delta = 0.215, b = 0.265$ . Parameters in the antiwave region remain the same:  $\delta = 0.146, b = 0.37$ . The arrows point to the direction of the phase velocity, same as Fig. 1.

so the corresponding parameter  $a$  was fixed on both sides to be 9.0. Parameter  $\delta$  on the two sides were different because the color concentration of the indicator were different. A small  $\delta$ , which corresponds to a high concentration of PVA, provided the antiwave area, while a large  $\delta$  provided the normal wave area. Considering the concentration of PVA ( $S$ ) is around  $4g/L \approx 10^{-4}M$ , and  $K$  is around  $6 \times 10^4$ ,  $\delta$  can be calculated to be about 0.15. In the simulation,  $\delta$  in the antiwave area was fixed at 0.146, and  $\delta$  in the normal wave area was used as a control parameter. The parameter  $b$  is also different on the two sides because a higher color indicator concentration corresponds to a lower iodine concentration. We calculated that  $b$  was in the range of  $0.25 \sim 0.33$ .

In the simulation study, we inserted values for the control parameters based on the above estimates, and used Eqn. (2) to conduct the simulations. Because different values of  $\delta$  led to different diffusion coefficients for variable  $x$  at the interface, the diffusion coefficient at the interface was set by taking the average of the two sides. This guarantees a continuous concentration and flux value across the interface. This boundary condition proved to be valid in CGLE simulations[9, 10]. The simulation results are shown in Fig. 3, which indeed shows three types of wave-antiwave interactions at the interface, as observed in the experiments. When the parameters on the normal wave side were  $\delta = 0.221, b = 0.32$ , the simulation gave an uncoupled state [Fig. 3(a), movie online].



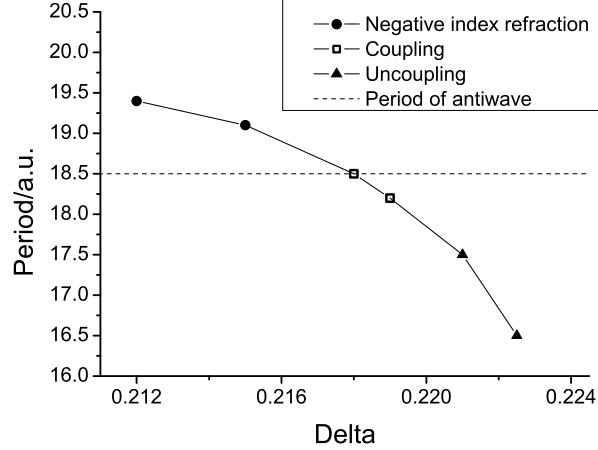


FIG. 4: The oscillating period of the normal wave in the RD system as a function of  $\delta$ . The area is divided into three parts: uncoupling state (triangles,  $\delta = 0.2225, b = 0.326$  and  $\delta = 0.221, b = 0.32$ ); wave-wave coupling state (squares,  $\delta = 0.219, b = 0.285$  and  $\delta = 0.218, b = 0.28$ ); negative index refraction (circles,  $\delta = 0.215, b = 0.265$  and  $\delta = 0.211, b = 0.258$ ). The dashed horizontal line marks the oscillation period of the antiwave.

As the parameters on the normal wave side were varied to  $\delta = 0.218, b = 0.28$ , waves became coupled [Fig. 3(b), movie online]. When the parameters on the normal wave side were below  $\delta = 0.215, b = 0.265$ , negative index refraction began to form [Fig. 3(c), movie online]. Thus, we demonstrated a quantitative agreement between experimental observations and numerical simulations.

We measured the oscillation period of the normal wave as a function of  $\delta$  and  $b$ . The result is shown in Fig. 4. One observes that the oscillation period increases as  $\delta$  decreases. The system shows uncoupling state, coupling state, and negative index refraction state in sequence as the oscillation period of the normal waves increases. The transition between the wave coupling state and the negative index refraction state takes place at the equal period line, which is consistent with our speculation. The critical value of  $\delta$  on the boundary between the uncoupled and coupled states reflects the discrepancy between the periods in the normal wave and antiwave wave regions. If the discrepancy is large, the resonance of the two waves stops so that there is no interaction between the two waves, as observed in the experiments.

In summary, we experimentally proved that a negative index of refraction phenomenon can occur in reaction-diffusion systems at the interface between a normal wave and an antiwave. The frequency of the normal wave being lower than that of the antiwave is a necessary condition.

This behavior in nonlinear waves is qualitatively different from the linear system, such as that of electromagnetic waves. In a nonlinear system that supports traveling waves, wave competition based on oscillation frequency is universal. The existence of and conditions for negative index refraction provide new insight in understanding the behavior of nonlinear traveling waves, which helps to explain wave propagation in macro structures, such as heart muscles and microorganisms.

### Acknowledgments

This work is partially supported by the NSF of China (10721403, 10774008, 11074009) and the MOST of China (2009CB918500).

- 
- [1] V.K. Vanag and I.R. Epstein, *Science* **294**, 835 (2001).
  - [2] V.K. Vanag and I.R. Epstein, *Phys. Rev. Lett.* **88**, 088303 (2002).
  - [3] X. Shao, Y.B. Wu and J.Z. Zhang, H.L. Wang and Q. Ouyang, *Phys. Rev. Lett.* **100**, 198304 (2008).
  - [4] H. Skødt and P.G.Sørensen, *Phys. Rev. E* **68**, 020902(R) (2003).
  - [5] J. Wolff, M. Stich, C. Beta and H.H. Rotermund, *J. Phys. Chem. B* **108**, 14282 (2004).
  - [6] A. Rabinovitch, M. Gutman and I. Aviram, *Phys. Rev. Lett.* **87**, 084101 (2001).
  - [7] C. Wang, C.X. Zhang and Q. Ouyang, *Phys. Rev. E* **74**, 036208 (2006).
  - [8] R. Zhang, L.F. Yang, A.M. Zhabotinsky and I.R. Epstein, *Phys. Rev. E* **76**, 016201 (2007).
  - [9] Z. Cao, H. Zhang, and G. Hu, *Europhys. Lett.* **79** 34002 (2007).
  - [10] X. Huang, X. Cui, Z. Cao, X. Liao, H. Zhang, and G. Hu, *Commun. Theor. Phys.* **52** 128 (2009).
  - [11] V.G. Veselago, *Sov. Phys. Usp.* **10**, 509 (1968).
  - [12] S. Yang, J.H. Page, Z. Liu, M.L. Cowan, C.T. Chan and P. Sheng, *Phys. Rev. Lett.* **93**, 024301 (2004).
  - [13] X.J. Yuan, X. Shao, H.M. Liao and Q. Ouyang, *Chin. Phys. Lett.* **26**, 024702 (2009).
  - [14] X.J. Yuan, X.C. Lu, H.L. Wang and Q. Ouyang, *Phys. Rev. E* **80**, 066201 (2009).
  - [15] Q. Ouyang and H.L. Swinney, *Nature* **352**, 610 (1991).
  - [16] Q. Ouyang and H.L. Swinney, *Chaos* **411**, 1 (1991).
  - [17] I. Lengyel, G. Rabai and I.R. Epstein, *J. Am. Chem. Soc.* **90**, 7683 (1990).
  - [18] I. Lengyel and I.R. Epstein, *Science* **251**, 650 (1991).
  - [19] I. Lengyel, S. Kadar and I. R. Epstein, *Phys. Rev. Lett.* **69**, 2729 (1992).

- [20] X. Shao, Y. Ren, and Q. Ouyang, Chin. Phys. B **15** 513 (2006).
- [21] B. Rudovics, E. Barillot, P.W. Davies, E. Dulos, J. Boissonade, and P. De Kepper, J. Phys. Chem. A **103**, 1790 (1999).
- [22] I. Lengyel and I.R. Epstein, Physica D **84**, 1-11 (1995).